2007-01-2260

An Explanation for Brake Groan Based on Coupled Brake-Driveline System Analysis

Ashley R. Crowther, J. Yoon, R. Singh
Acoustics and Dynamics Laboratory, The Ohio State University

ABSTRACT

Brake creep-groan is studied via a friction coupled torsional model consisting of driveline and brake sub-systems. The model captures the main torsional modes of interest while a suitable reduction of higher degree-of-freedom models allows selection of appropriate parameters. Numerical simulations are programmed that capture groan response with stick-slip friction and transient brake pressure. The vehicle is initially at rest and the groan may build into a steady state limit cycle, depending on the brake force actuation. For automatic transmission (AT) the driving torque is at the torque converter. For manual transmission (MT) the vehicle is on a slope and the driving torque is due to weight of the vehicle. On-vehicle tests provide time and frequency domain measured accelerations for comparison.

INTRODUCTION

Creep-groan may occur as a vehicle starts to move from rest. For AT vehicles the torque converter impeller is applying small torque on the stationary turbine and hence the rest of the powertrain. The driver may wish to slowly move some small distance and stop (e.g. in stop-go traffic, at traffic lights, in garage maneuvers). With slow pedal release the brake friction torque will be overcome by the driving torque (impeller) and the brake rotor will start to slip against the brake pad. This initial slip excites vibration of the driveline and brake sub-systems, allowing a condition where the rotor and pad may stick again. In practice this stick-slip motion may repeat until the rotor and pad reach some steady-sliding state, or stick and halt the vehicle. The motion is highly dependent on pedal actuation. For MT the vehicle is on a slope, with clutch disengaged and the driver is easing the car from rest. The reasons for the onset of groan are similar but the driving torque is due to weight of the vehicle. In theoretical models, depending on conditions, it can be shown to repeat forever in a stick-slip limit cycle. Many parameters affect this creep-groan phenomenon, including, but not limited to, system modes, damping, friction characteristics, driving torque magnitude, rate and magnitude of brake release, rate and magnitude of brake reapplication and hydraulic system dynamics. Groan may also occur on brake application as reported by Brecht [1]; it typically can be a long event for brake release on takeoff and a short event for vehicle braking to stop. Jang et al. [2], suggest approaches to minimize the vibration by increasing damping or inertia of the rotating bodies and by reducing system compliance. The problem is related to many in the large body of literature for friction research, Martins et al. [3] give a lengthy review that includes most relevant material.

The brake creep groan problem remains a complex engineering problem that has yet to be fully understood or analyzed. We propose an analytical investigation of four-degree-of-freedom torsional model (as shown in Figure 1). It includes driveline and brake torsional sub-systems, with friction interface through the brake rotor and pad. This model should conceptually describe the brake creep-groan phenomenon and several types of stick-slip motions, and yet it could be easily extended. Note that two dynamic sub-systems are coupled by a friction interface, an important aspect of the non-linear model (as illustrated by Figures 1-2). The frequency ratio for the sub-system modes dominating the stick-slip motions is not near zero (or infinite), hence neither the brake or powertrain sub-systems may be considered as a rigid body. Specific objectives of this paper are as follows: a) Demonstrate the model of two dynamic sub-systems coupled with friction interface for the brake groan problem; b) Describe briefly the identification of relevant system parameters; c) Formulate and obtain solutions to the creep-groan response for AT and MT cases; d) Conduct analogous vehicle experiments and show a preliminary correlation between theory and experiment.

BRAKE GROAN MODEL

The reduced order dynamic model of Figure 1 is designed so as to be applicable to a vehicle with either automatic or manual transmission. Further, it could be employed to study both transient and stick-slip periodic motions. Since brake groan is induced by the stick-slip phenomenon the equations of motion are given below in matrix form where the friction torque introduces a piecewise non-linearity:

$$\mathbf{J}\ddot{\boldsymbol{\theta}} + \mathbf{C}\dot{\boldsymbol{\theta}} + \mathbf{K}\boldsymbol{\theta} = \mathbf{T}(\dot{\theta}, t) \quad (1)$$

Here J, C and K represent inertia, damping and stiffness matrices respectively, T is the external torque vector and θ is the angular displacement vector. Under the slipping condition the governing system of Fig. 1 is of dimension four and is given by $\boldsymbol{\theta} = \{\theta_d \quad \theta_r \quad \theta_b \quad \theta_t\}^T$ and,

$$\mathbf{J} = diag\left[J_d \;\; J_r \;\; J_b \;\; J_t\right]; \mathbf{K} = \begin{bmatrix} k_d & -k_d & 0 & 0 \\ -k_d & k_d + k_t & 0 & -k_t \\ 0 & 0 & k_b & 0 \\ 0 & -k_t & 0 & k_t \end{bmatrix};$$

$$\mathbf{C} = \begin{bmatrix} c_d + d_d & -c_d & 0 & 0 \\ -c_d & c_d + c_t & 0 & -c_t \\ 0 & 0 & c_b & 0 \\ 0 & -c_t & 0 & c_t + d_t \end{bmatrix}; \; \mathbf{T} = \begin{bmatrix} T_d \\ -T_b \\ T_b \\ -T_v \end{bmatrix}. \quad (2a\text{-}d)$$

The viscous damping is introduced via *c* terms along with stiffness elements and inertial damping terms, d_d and d_t, applied on the powertrain equivalent inertia and tire/vehicle inertia. Under the sticking condition the dimension of Fig. 1 is reduced by one, giving, $\boldsymbol{\theta} = \{\theta_d \quad \theta_{r/b} \quad \theta_t\}^T$, where $\theta_{r/b}$ indicates brake and rotor coordinates, and

$$\mathbf{J} = diag\left[J_d \;\; J_r + J_b \;\; J_t\right]; \; \mathbf{K} = \begin{bmatrix} k_d & -k_d & 0 \\ -k_d & k_d + k_t + k_b & -k_t \\ 0 & -k_t & k_t \end{bmatrix};$$

$$\mathbf{C} = \begin{bmatrix} c_d + d_d & -c_d & 0 \\ -c_d & c_d + c_t + c_b & -c_t \\ 0 & -c_t & c_t + d_t \end{bmatrix}; \mathbf{T} = \begin{bmatrix} T_d \\ k_b \hat{\delta} \\ -T_v \end{bmatrix}. \quad (3a\text{-}d)$$

By reduction of a more detailed model the parameters for the driveline sub-system are established for a typical mid-sized RWD automatic transmission (AT) vehicle (see [4] for more details). The detailed model of Fig. 3 allows selection of inertias, engine/flywheel/torque converter, rotating transmission elements, final drive pinion and ring (crown wheel), hub/brake rotor and vehicle. By appropriate reduction where significant stiffness elements are combined in series or parallel we obtain:

$$k_d = \left[\frac{2}{n_{fd}^2 k_{eq1}} + \frac{1}{k_a}\right]^{-1}, \quad (4a)$$

where $k_{eq1} = 0.5\left[\frac{1}{n_{tr}^2 k_{is}} + \frac{1}{k_{os}} + \frac{1}{k_{ps}}\right]^{-1}$.

Likewise, inertias are combined as,

$$J_d = 0.5\left[n_{tr}^2 n_{fd}^2 \left(J_e + J_{tc} + J_{tr1}\right) + n_{fd}^2 \left(J_{tr2} + J_{fd1}\right) + J_{fd2}\right]. \quad (4b)$$

Note that only one braking wheel is considered, thus the half term is applied above; also $J_t = J_{tr}$ and $k_a = k_{ar}$ and $k_t = k_{tr}$. Engine torque is now expressed as drivetrain torque applied at the final drive output:

$$T_d = 0.5 n_{tr} n_{fd} T_e. \quad (4c)$$

For reference, transmission and final drive speed ratios are $n_{tr} = 2.4$ and $n_{fd} = 3.2$. Ballpark parameters for the brake system were established via modal testing and system identification [4]. Of several low frequency modes, the lowest torsional mode of the brake knuckle and suspension was identified and used to determine an effective torsional stiffness. The reduced system parameters are given with the Figure 3 caption.

When slipping the system has a rigid body mode of rotation and three damped frequencies, $f_{di}^{SL} = 4.3,\ 34.5,\ 95.4$ Hz; the first mode is global and the second and third modes describe localized rotor and brake motions, respectively. The damping ratios are $\xi_i^{SL} = 0.05,\ 0.05,\ 0.02$. For sticking the brake and rotor inertias are combined and $f_{di}^{ST} = 2.4,\ 4.6,\ 54.6$ Hz; the first and second modes are global and the third modes describe the coupled brake-rotor motion. The damping ratios are $\xi_i^{SL} = 0.095, 0.045,\ 0.033$.

FRICTION LAW

The brake torque is a function of the average radius of contact, r_b, between the brake pad and rotor and brake friction force, $F_b\left(\dot{\delta}, t\right)$, as shown in Figure 1c. A key simplifying assumption is that the brake friction force is described with Coulomb's law with both static and kinetic friction coefficients, μ_s and μ_k. Figure 2 illustrates the friction law for an instantaneous or constant value of the brake normal force, $F_n(t)$. With consideration of the direction of sliding and the sticking regime, the brake friction torque may be expressed as follows with a piecewise function in terms of the slipping angular velocity, defined as $\dot{\delta} = \dot{\theta}_r - \dot{\theta}_b$:

$$T_b = \begin{cases} r_b \mu_k F_n & \dot{\delta} > 0 \\ r_b \mu_s F_n & \dot{\delta} = 0^+ \\ T_b^{ST} & \dot{\delta} \equiv 0 \\ -r_b \mu_s F_n & \dot{\delta} = 0^- \\ -r_b \mu_k F_n & \dot{\delta} < 0 \end{cases}, \quad (5)$$

Further definitions include, $T_b^{SL} = \pm r_b \mu_k F_n$, the slipping friction torque, $T_b^B = \pm r_b \mu_s F_n$, the breakaway friction torque (or threshold) and T_b^{ST}, the actual sticking torque or the shear torque between sticking elements during sticking motions.

The slipping condition is for all *t* where $|\dot{\delta}| > 0$ and the sticking condition is for all *t* where $\dot{\delta} \equiv 0$. The stick to slip transition occurs at the instant when the sticking friction torque exceeds the breakaway torque:

$$|T_b^{ST}| > |T_b^B| = r_b \mu_s F_n . \quad (6)$$

At some instantaneous time, *t*, the motions may be at the stick-slip boundary, which is defined by the following, where $\dot{\delta} = 0^{\pm}$:

$$|T_b^{ST}| = |T_b^B| = r_b \mu_s F_n . \quad (7)$$

Crossing the boundary from the sticking regime requires only that (6) be satisfied. Crossing the boundary from the slipping regime requires both:

$$\dot{\delta} = 0^{\pm} \text{ and } |T_b^{ST}| \le |T_b^B| = r_b \mu_s F_n . \quad (8a,b)$$

Finding the exact intersection point, $\dot{\delta} \equiv 0$, for the above condition is impractical, whether solving via numerical integration or when assembling piecewise analytical solutions. Various approaches such as bisection methods require a small bracket within which a value close to zero may be taken as zero. We illustrate this bracket in Figure 2, which is referred to as the zero velocity tolerance:

$$\dot{\delta} = 0 \text{ where } \dot{\delta} = \{-\varepsilon_{\dot{\delta}} \le 0 \ge \varepsilon_{\dot{\delta}}\}. \quad (9)$$

In our simulations we apply a time-varying tolerance as a function of the slope of relative velocity, see [4] for details.

SIMULATION OF GROAN EVENTS FOR AUTOMATIC TRANSMISSION

The nature of the instance of creep-groan is dependent on the transmission type. For AT the vehicle is at rest and the drivetrain loaded then as the brake is released the rotor slips against the driving torque converter. For this case, simulations are performed where at $t = 0s$, all inertias are at rest and a small constant torque is applied at the drive. The brake normal force is then decreased for $t \ge 0s$, leading to rotor slip and creep-groan. Solutions to Equation (1) are found in a piecewise manner as governed by the friction laws (6, 8). Further, the engine torque is assumed as $T_e = 20\,\mathrm{Nm}$, which for the reduced model (Figure 1) gives a drive torque, $T_d = 76.8\,\mathrm{Nm}$. Parameter d_t provides a drag torque of $-d_t \dot{\theta}_t\,\mathrm{Nm}$ (2c, 3c), simplifying rolling resistance and friction. The road gradient is assumed as 0° so for this case $T_v = 0$ Nm.

The brake force is modelled with a hyperbolic tangent function with positive mean part, $F_n(t) = F_m - \beta \tanh \sigma t$ (Figure 4a). The rate and magnitude of release may be controlled with τ and β parameters. $\hat{F}_n = T_d / r_b \mu_s$ is the brake slip line and $F_n(t) = \hat{F}_n$ gives initial slip. The initial torque vector is $\mathbf{T}(0) = [T_d \;\; 0 \;\; 0]^T$ where at rest and under sticking condition the initial conditions are $\boldsymbol{\theta}(0) = \mathbf{K}^{-1}\mathbf{T}(0)$ and $\dot{\boldsymbol{\theta}}(0) = 0$, with system matrices (3a-d) and coordinate vector $\boldsymbol{\theta} = \{\theta_d \;\; \theta_{r/b} \;\; \theta_t\}^T$.

The numerical solver is a Runge-Kutta 2,3 method [5] with adaptive step size control. The governing equations are defined in the reduced (first order) form, $\dot{\mathbf{U}} = \mathbf{B}\mathbf{U}$, where $\mathbf{U} = \{\theta_d \;\; \theta_r \;\; \theta_b \;\; \theta_t \;\; \dot{\theta}_d \;\; \dot{\theta}_r \;\; \dot{\theta}_b \;\; \dot{\theta}_t\}^T$.

For slipping, the accelerations, $\dot{\mathbf{U}}_i(t_n)$, $i = 5 \text{ to } 8$, are determined for (1) with (2a-d). Retaining four degrees-of-freedom while sticking simplifies programming, and hence the expanded form of (1) is used with (3a-d). The sticking brake and rotor move together as governed by the following equation:

$$\ddot{\theta}_{r/b} = \frac{1}{(J_r + J_b)} \begin{bmatrix} c_d(\dot{\theta}_d - \dot{\theta}_r) - c_t(\dot{\theta}_r - \dot{\theta}_t) - c_b \dot{\theta}_b + \\ k_d(\theta_d - \theta_r) - k_t(\theta_r - \theta_t) - k_b \theta_b \end{bmatrix} \quad (10)$$

We present one example case where $\tau = 0.4$ and $\beta = 30$N give the brake force of Figure 4a. Here the friction coefficients are $\mu_k = 0.4$, $\mu_s = 0.6$ and the brake radius, $r_b = 0.12$ m. While sticking the brake torque is:

$$T_B^{ST} = (1-\Gamma)\begin{bmatrix} c_d(\dot{\theta}_d - \dot{\theta}_r) - c_t(\dot{\theta}_r - \dot{\theta}_t) + \\ k_d(\theta_d - \theta_r) - k_t(\theta_r - \theta_t) \end{bmatrix} + \Gamma[c_b\dot{\theta}_b + k_b\theta_b] \quad (11)$$

Where $\Gamma = J_r/(J_r + J_b)$ is an inertia ratio. During the initial slip the brake/rotor velocity (Figure 4b) jumps abruptly leading to a transient groan followed by steady-state (sustained) groan. The vehicle displacement after 200ms of creep-groan (stick-slip) is approximately 50mm (or 6° of wheel rotation). If the brake force is released enough the groan can abruptly cease for steady brake sliding (and significant forward motion of the vehicle). If enough pressure is further applied the brake will lock and motions will cease

The orbit for the stick-slip motions (Figure 5) is one of several types we found for a range of parameters β and τ [6]. Figure 6 shows the brake torque, brake/rotor relative velocity and their accelerations. Referring Figure 6a, while sticking, the brake torque is T_b^{ST} and the slipping velocity, $\dot{\delta} = 0$ (Figure 6b). The brake slips when the sticking torque exceeds the breakaway torque, $|T_b^{ST}| > |T_b^B|$. The torque is now the slipping value, T_b^{SL}. When $\dot{\delta} = 0$ next occurs, the brake and rotor stick as long as $|T_b^{ST}| \le |T_b^B|$ and the cycle repeats. The orbits demonstrate sticking, τ^{ST}, slipping, τ^{SL} and stick-slip, τ^{SS} periods. In Figures (6c-d) the accelerations of the rotor and the brake show jumps on stick-slip and slip-stick transitions.

SIMULATION OF GROAN EVENTS FOR MANUAL TRANSMISSION

The model of Figure 1 can similarly be applied to a manual transmission vehicle. Figure 7 shows the reduction steps. The transmission is a four-speed single-stage constant mesh. The gearbox is combined with final drive hence the entire unit is a 'transaxle'. For simplicity, the lay shaft carries all dog clutches and on the primary shaft the gears are always fixed. In 1st gear the 1-2 dog clutch engages the 1st gear to the lay shaft. The reduced inertias are summed and the stiffness combined in series (accounting for gear ratio) to give drive inertia and stiffness:

$$J_d = 0.5\left[n_{fd}^2 n_{tr}^2 (J_c + J_{tr1}) + n_{fd}^2 (J_{tr2} + J_{fd1}) + J_{tr2}\right], \quad (12a)$$

$$k_d = \left[\frac{2}{n_{fd}^2 k_{eq1}} + \frac{1}{k_a}\right]^{-1}, \quad (12b)$$

Where,

$$k_{eq1} = \left[\frac{1}{n_{tr}^2 k_p} + \frac{1}{k_l}\right]^{-1}.$$

The speed ratios are transmission, $n_{tr} = 3.45$ and final drive, $n_{fd} = 3.88$. The new system parameters give slipping damped frequencies, $f_{di}^{SL} = 9.57, 33.1, 95.4$ Hz and for sticking, $f_{di}^{ST} = 2.4, 10.4, 53.7$ Hz. Notice that the first slipping mode and second sticking modes have increased significantly. They are the same global drivetrain mode. The inertia ratio, Γ, is unchanged and considering the linear homogeneous system the principle difference with the MT formulation is the decoupling of the engine.

For simulation we figuratively place the vehicle on an inclined road and its weight, *W*, is held by the brake force. Assumptions include equal weight distribution amongst four contact points (tires) and no slipping (pure rolling contact). The weight expressed as the apportion of torque applied to one tire:

$$T_v = 0.25 r_t W \sin\varphi \quad (13)$$

Where r_t is the tire radius and φ the road slope. The disengaged clutch gives drive torque, $T_d = 0$ and the vehicle is assumed to be 1500kg. For sake of comparison, similar forcing conditions to the AT simulation can be achieved; selecting $\varphi = 16.86°$ gives $T_v = 76.8$Nm, for the AT simulation this value was for T_d. However, this constant 'driving' force is now applied at the tire inertia rather than drive inertia. The brake force transient and brake slip line are identical to Figure 4a. Initial conditions are similarly calculated; the initial twist must leave the system motionless until the slip line is crossed.

Figure 8 gives the brake/rotor relative velocity, first notice the transient region is shorter than for the AT vehicle. This may be as the driving force is now through the 'heavy' tire inertia (reflective of vehicle mass), whereas for the AT vehicle the driving force is on the much 'lighter' drive inertia. Maximum slipping velocity is of similar order in each case, however the periodicity of the stick-slip orbit is markedly different. The phase planes (Figure 9) show brake/rotor relative motions having three stops per period. Each of the three stick-slips has similar time durations within the period. A sizable parameter variation study [6] for the AT system has only shown one-stop (such as Figure 5). However there were three different motion types with one-stop. A deeper understanding of behavior under the MT forcing conditions could be gained from similar studies. The rotor shows motion in a similar range to the brake and evidently the driveline sub-system is playing a significant part in the motion. The effect of drive inertia (or ignoring it), tire stiffness, slope, inertia and frequency ratio could also be examined.

VEHICLE GROAN EXPERIMENT

A typical medium sized passenger vehicle (with AT) is used to measure typical characteristics of brake groan. The tests duplicate the driver behavior of creeping forward in almost stationary traffic or at traffic lights; a condition where creep-groan is common. The vehicle is stationary on flat ground, the engine is idling and the applied brake is resisting a small amount of torque from the torque converter. The driver releases the brake very slowly until groan occurs and with careful actuation of the brake pedal the recording of sustained groan events is possible. The noise is measured at the driver's right ear position and atop the wheel arch 100mm away from the vehicle body. Two accelerometers (Figure 10) are mounted on the brake caliper and suspension strut. The brake caliper accelerometer measures motion near tangential to the pad contact area on the brake rotor, the suspension strut accelerometer measures fore-aft motions. Data is sampled at 48,000 Hz. Tests run for around 60s with the driver repeating the process of inducing 0.5-2s groans up to 15 times a test. That the wheel rotates no more than 30° over 60s illustrates the very low speed range for creep-groan.

Experimental results show the nature of the transient events and also provide some steady-state groan data. For instance, Figure 11 illustrates multiple intermittent brake groan events in terms of measured acceleration. Here the groan events are labeled A to I. Events A, B, E and G are where the driver releases the brake only slightly past the point of initial slip and then re-applies giving a short "creak" sound, rather than sustained groan. Figure 12 provides a close up look of event B; evident is an impulse, or two, followed by a decay transient with rich spectra. Events C ,D, F, H and I show a more continuous repetition of these impulses and decay transients over a finite duration. Focusing on event F in Figure 13, the groan is first transient (t = 19.8 – 20.6s), then progresses to an almost steady state for 1s (t = 20.6 – 21.6s). The groan dies away fairly abruptly at about 22.1s. During the steady state region the impulses occur at approximately 75 Hz.

We can examine the frequency spectra for Events A to I by taking the short time FFT and construct waterfall plots showing the time-frequency content. Due to the transient nature of the sample set the FFT process will have an averaging effect on frequencies and amplitudes, however this does not effect the illustrative purpose of such examination. Figure 14 shows such time-frequency characteristics for the five major groan events C, D, F, H and I. For each event, the variation in brake pressure leading to groan would be different, depending on how the driver actuated the pedal. The length and mean-square quantities are also different, yet the main frequency stays within a fairly narrow band of 76 Hz, which may be the stick-slip frequency. The harmonics are related to the friction discontinuity. The results show a preliminary correlation between theory and experiment. The stick-slip impulses are seen in both simulated (Figure 6c-d) and measured accelerations (Figure 13). There is a comparable sudden onset and cessation of groan.

CONCLUSION

In this paper we studied a particular problem for a ground vehicle system using analytical and numerical methods. Our analysis reveals that the impulsive and discontinuous nature of stick-slip motions between rotor and disc is the source of creep-groan and it can be either transient or steady state. For MT or AT vehicles the problem may be formulated into identical torsional-spring mass models with appropriate parameters derived from models with higher degrees-of-freedom. The model and numerical methodology allow the study of many sensitive parameters; inertia and frequency ratio, rate and magnitude of transient brake force, friction ratio, etc.

[1] Brecht J., Hoffrichter W., Dohle A., *'Mechanisms of Brake Creep-groan'*, SAE Technical Paper **973026,** SAE 1997.

[2] Jang H., Lee J.S., Flash J.W., *'Compositional Effects of the Brake Friction Material on Creep-groan Phenomenon'*, Wear **251**, 2001, 1477-1483.

[3] Martins, J.A.C., Oden J.T., Simoes, F.M.F., *'Recent Advances in Engineering Science – A Study of Static and Kinetic Friction'*, International Journal of Engineering Science **28(1)**, 1990, 29-92.

[4] Crowther A.R., Singh R., *'Analytical Investigation of Stick-Slip Motions in Coupled Brake-Driveline Systems'*, Journal of Non-Linear Dynamics (accepted for publication October 2006).

[5] Bogacki P., Shampine L.F., *'A 3(2) Pair of Runge-Kutta Formulas'*, Applied Mathematics Letters **2**, 1989, 1-9.

[6] Crowther A.R, Singh R., *'Identification and Quantification of Stick-Slip Induced Brake Groan Events Using Experimental and Analytical Investigations'*, to be submitted to the Noise Control Engineering Journal.

CONTACT

A.R. Crowther and R. Singh, Acoustics and Dynamics Laboratory, Mechanical Engineering Department, The Ohio State University, Columbus, OH 43210, USA, Phone: +1 614-292-4147, Fax: +1 614-292-3163, crowther.5@osu.edu, singh.3@osu.edu

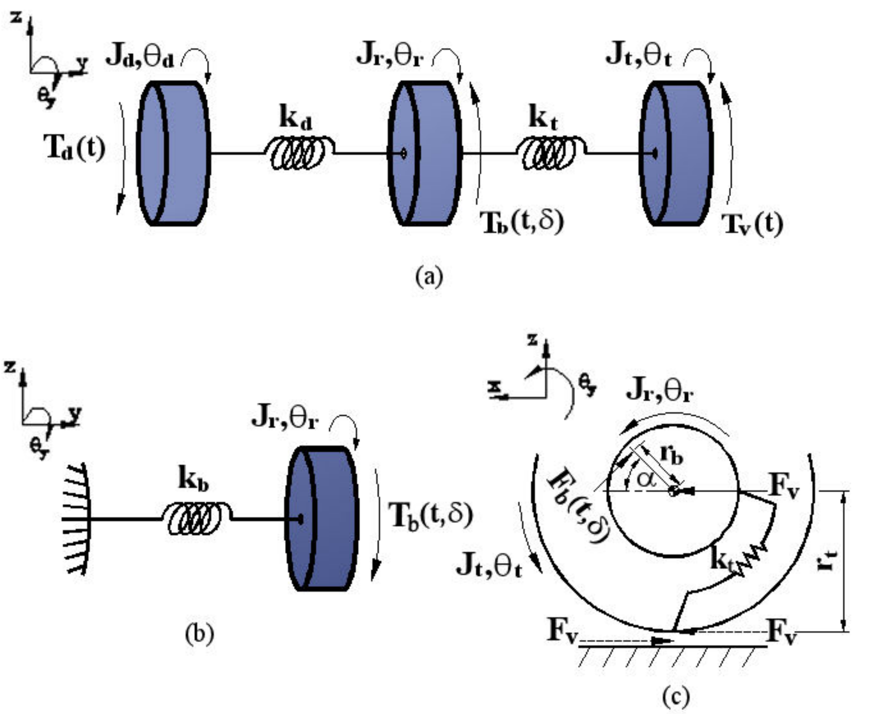

Figure 1: Torsional Model Utilized for Brake Groan Analysis: (a) Driveline Sub-system, (b) Brake Sub-system and (c) Rotor/Tire Side View.

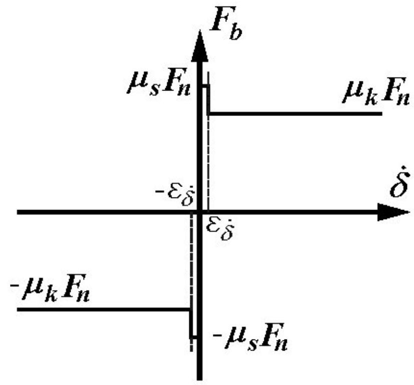

Figure 2: Brake Friction Force as a Function of Sliding Velocity

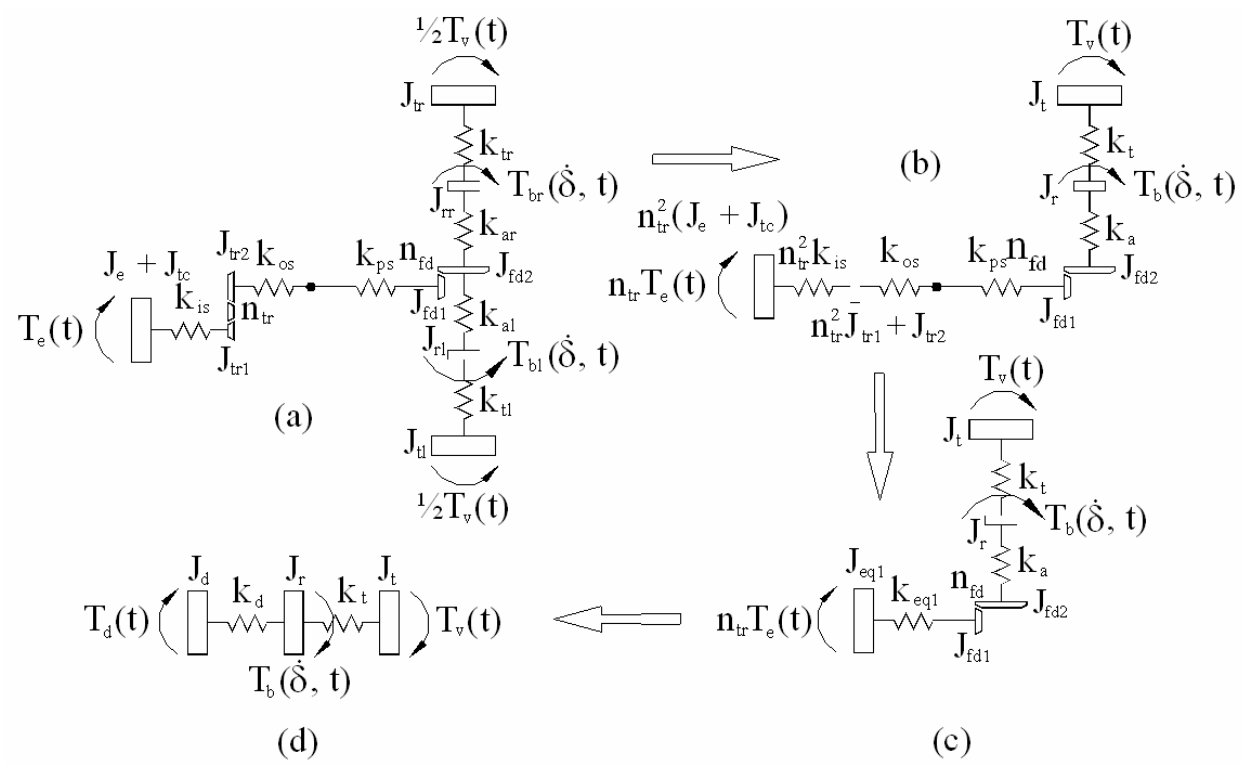

Figure 3: Driveline Model of a Vehicle with Automatic Transmission. Reduction of Torsional Models from (a) through Steps (b) and (c) and to Reduced Form (d). For System (d) Parameters are: Inertia, $J_d = 9.54$, $J_r = 0.65$, $J_b = 0.119$ and $J_t = 73.08$ (kgm²); Stiffness, $k_d = 8788$, $k_b = 68000$, $k_t = 22000$ (Nmrad^{-1}); Damping, $c_d = 1.15$, $c_b = 4.53$, $c_t = 13$, $d_d = 23.9$ and $d_t = 200$ (Nmsrad^{-1}).

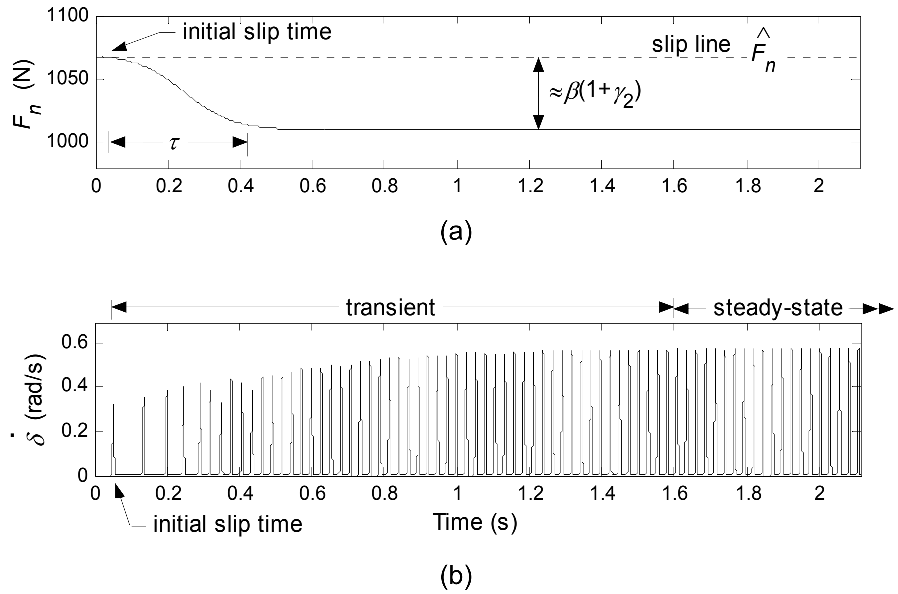

Figure 4: Simulation for Creep-Groan in an AT vehicle: (a) Brake Normal Force and Brake Slip Line; (b) Brake/Rotor Relative Velocity (Slipping Velocity) showing Transient Groan Leading to Steady-State Groan (Stick-slip Orbits).

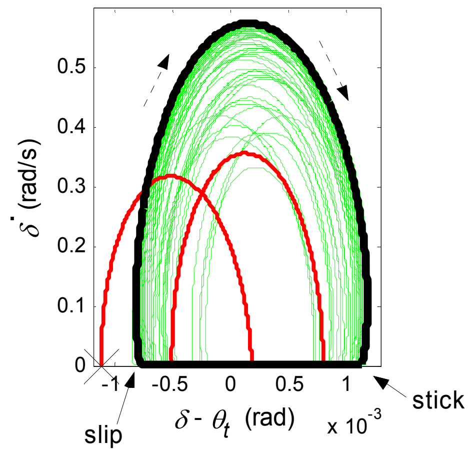

Figure 5: Phase Plane for Creep-Groan in an AT Vehicle. Key: X Marks Initial Conditions; Thick Line – Orbit.

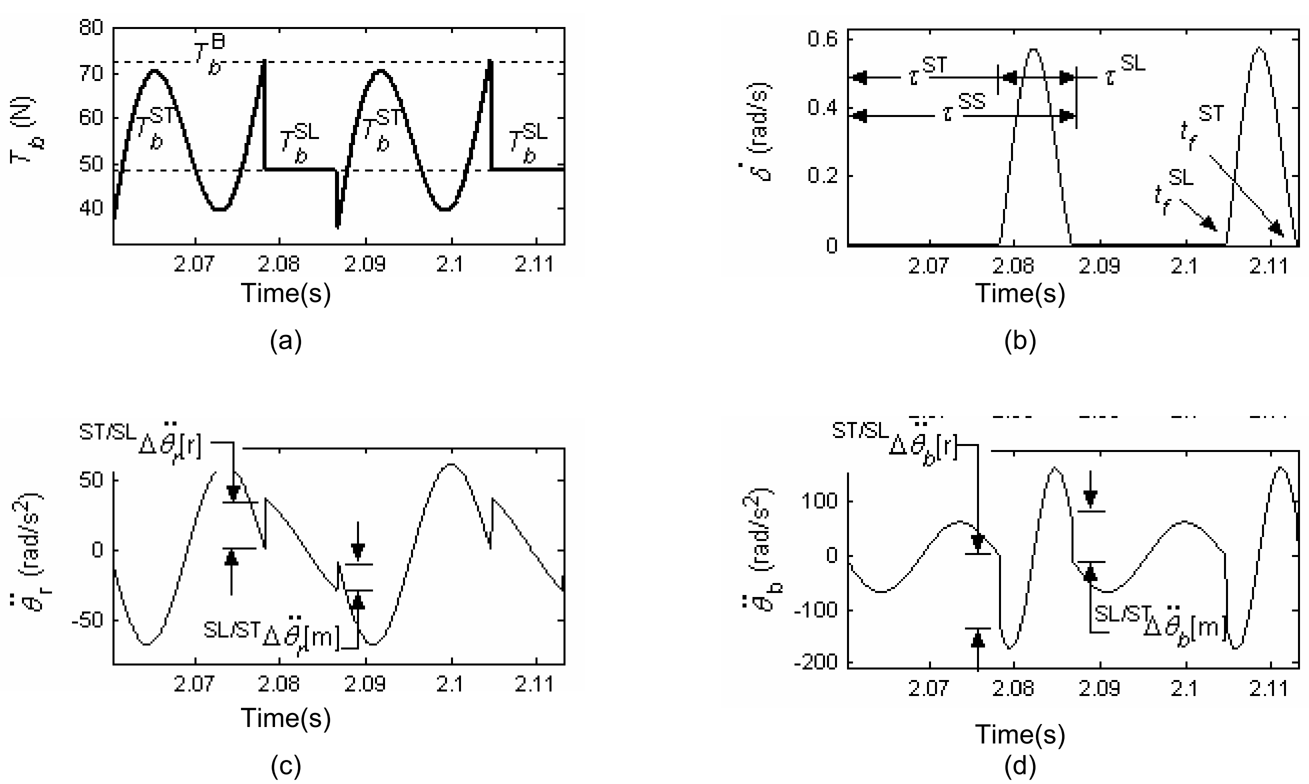

Figure 6: Two Cycles of Steady-State Response (Orbits) for Creep-Groan: (a) Brake Torque; (b) Slipping Velocity; (c) Rotor Acceleration; (d) Brake Accelerations.

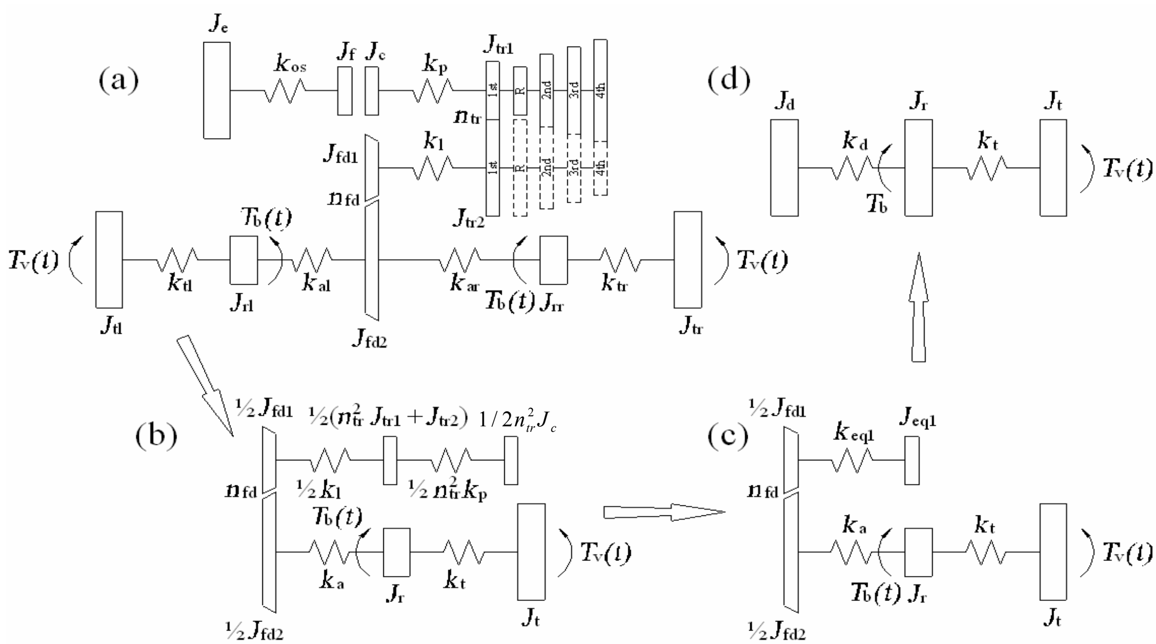

Figure 7: Driveline Model of a Vehicle with Manual Transmission: Reduction of Torsional Models from (a) through Steps (b) and (c) to Reduced Form (d). System Parameters are: Inertia, $J_d = 1.19$, $J_r = 0.65$, $J_b = 0.189$ and $J_t = 73.08$ (kgm^2); Stiffness, $k_d = 5385.8$, $k_b = 68000$, $k_t = 22000$ (Nmrad^{-1}); Damping, $c_d = 1.15$, $c_b = 4.53$, $c_t = 12.25$, $d_d = 6.14$ and $d_t = 600$ (Nmsrad^{-1}).

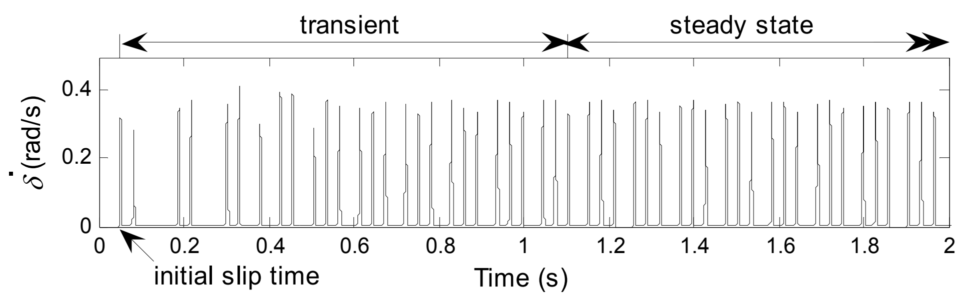

Figure 8: Simulation for Creep-Groan in an MT Vehicle: Result for Brake/Rotor Relative Velocity (Slipping Velocity) showing Transient Groan Leading to Steady-State Groan (Stick-slip Orbits)

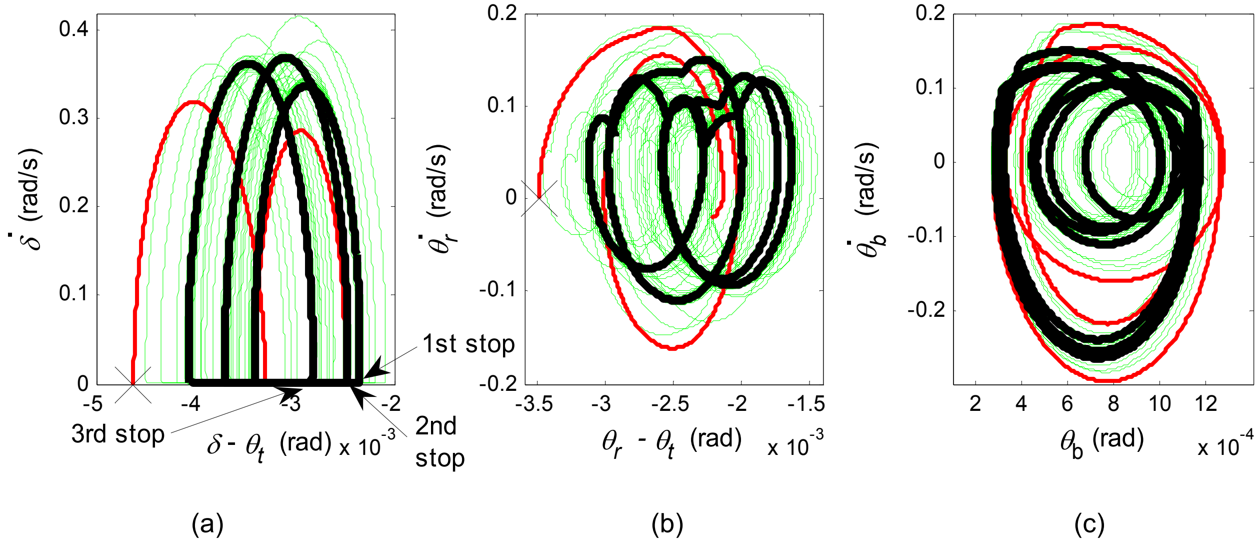

Figure 9: Phase Planes for Creep-Groan in an MT Vehicle: a) Brake/Rotor Relative Motion; b) Rotor Motion; c) Brake Motion. Key: X - Initial Conditions, Thick Line - Orbit.

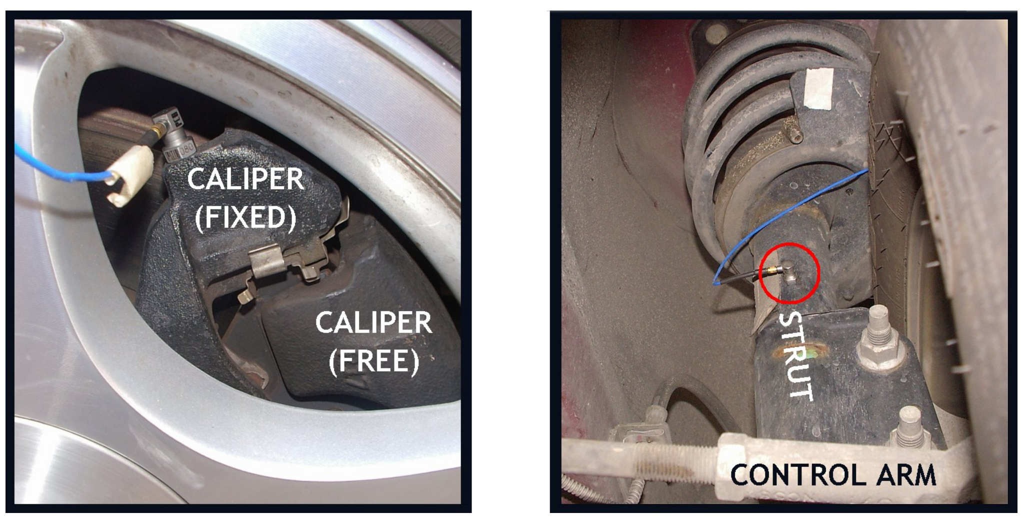

Figure 10: Accelerometer Locations for Creep-Groan Experiment.

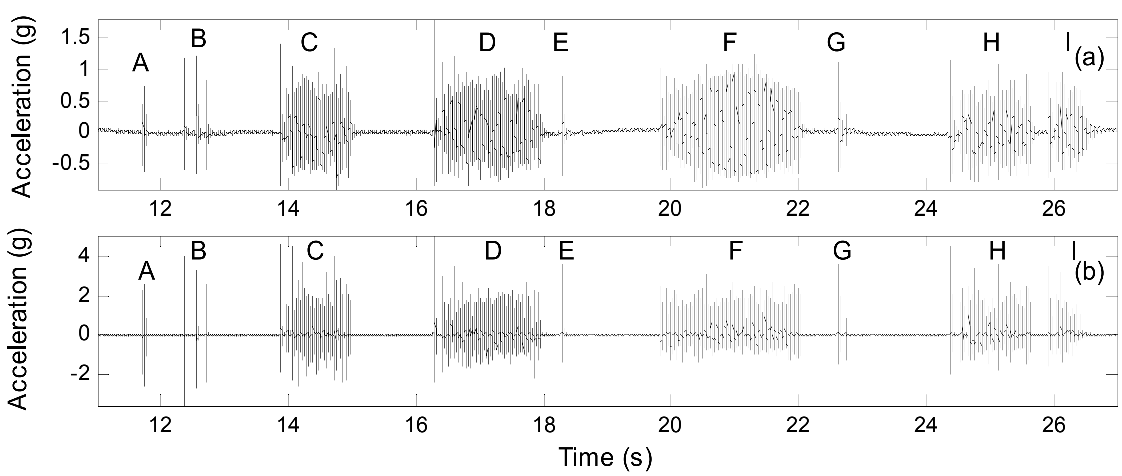

Figure 11: Measured Acceleration Time Histories for Intermittent Groan with Groan Events labeled A to I: a) Suspension Strut Fore-Aft Accelerometer; b) Caliper Tangential Accelerometer.

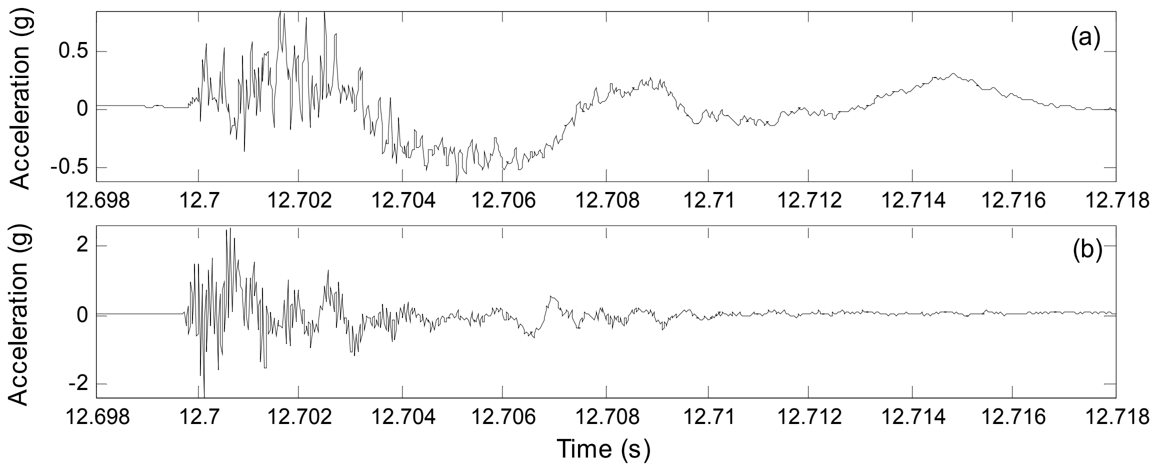

Figure 12: Event B: Time Histories for a) Suspension Strut Fore-Aft Accelerometer; b) Caliper Tangential Accelerometer.

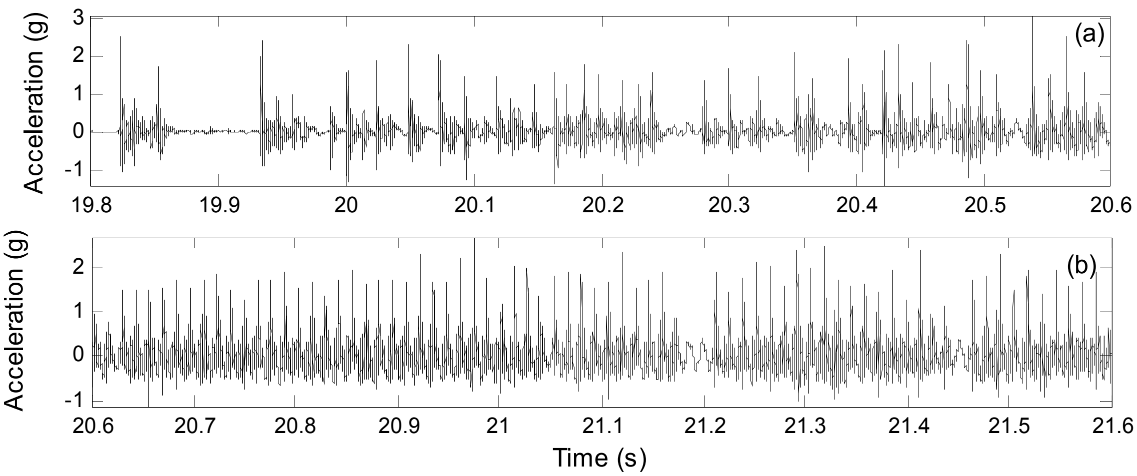

Figure 13: Event F: Time History for Caliper Tangential Accelerometer showing a) Transient Part Groan leading to b) Steady State Groan

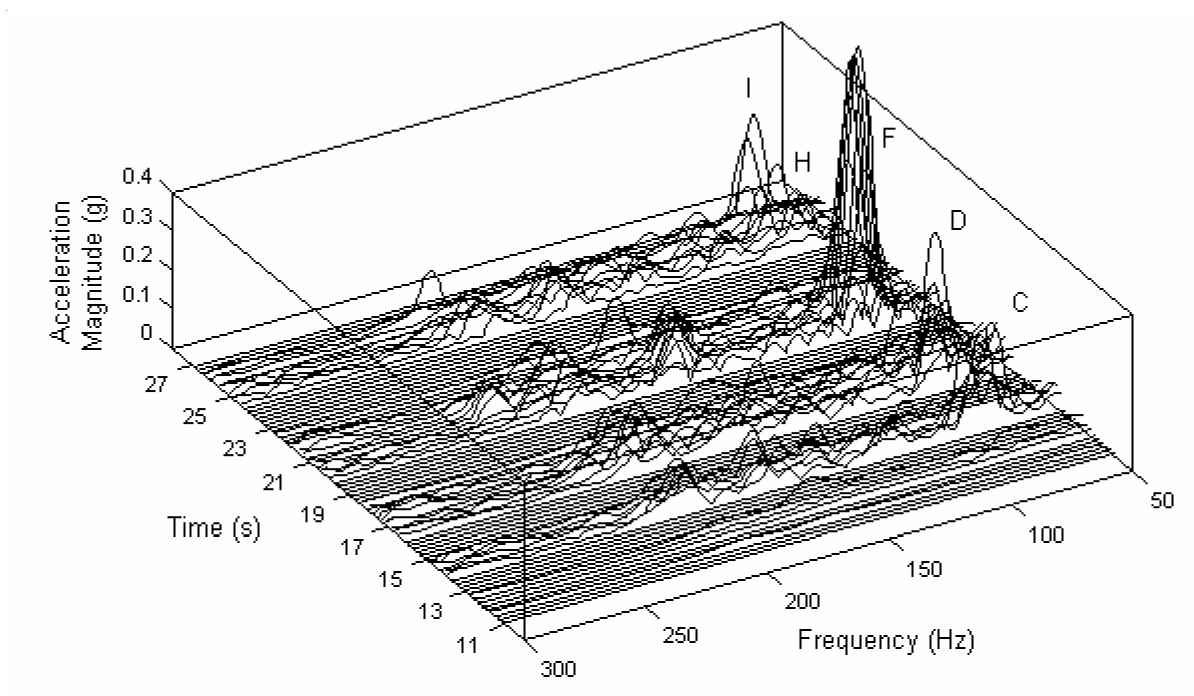

Figure 14: Waterfall Plot Showing ‘Averaged’ Frequency Content of Transient Groan Events A-I as Measured via Suspension Strut Fore-Aft Accelerometer.